ARTICLE

Embryological Development of *Caiman latirostris* (*Crocodylia*: *Alligatoridae*)

Josefina Iungman,[1,2] **Carlos I. Piña,**[1,2,3] **and Pablo Siroski**[2,4]*
[1]CICyTTP-CONICET, Dr. Materi y España, CP 3105, Diamante Entre Ríos, Argentina
[2]Proyecto Yacaré. Av. Aristóbulo del Valle 8700, CP: 3000, Santa Fe, Argentina
[3]UAdER, Fac. de Cs. y Tecnología. Subsede Diamante, Entre Ríos, Argentina
[4]Secretaría de Medio Ambiente de la Provincia de Santa Fe (MASPyMA), Santa Fe, Argentina

Received 18 December 2007; Revised 24 April 2008; Accepted 5 June 2008

Summary: A standard development embryological series is the primary basis to organize information of any embryological study and is also used to determine the age of eggs and embryos in field conditions. In this article, we calibrate developmental series of the broad-snouted caiman, *Caiman latirostris*, against an established series for *Alligator mississippiensis*. Morphometric measures and extend of the opaque-shell banding were also related to embryo age. In earlier stages, external morphological features alone can account for embryo age, but we suggest that morphometric measurements should be introduced later in the development. Unlike morphologic and morphometric attributes, the opaque patch was not a useful age predictor. As expected, a close correlation between embryonic development of *C. latirostris* and *A. mississippiensis* was observed. genesis 46:401–417, 2008. © 2008 Wiley-Liss, Inc.

Key words: broad-snouted caiman; embryology; incubation; growth

INTRODUCTION

Standard embryological series are the primary basis for organizing information of any embryological study, either descriptive or experimental (Beggs *et al.*, 2000; Hamburger and Hamilton, 1992; Hua *et al.*, 2004). It is also a useful means of studying ecological and evolutive aspects (Andrews and Mathies, 2000; Andrews, 2004), comparing embryos developing under different incubation conditions, and staging embryos or ageing clutches under field incubation conditions. In species whose differentiation depends, to a greater extent, on environmental conditions in which eggs are incubated, staging and ageing become particularly important. In fact, temperature has several effects on reptilian embryo differentiation, including development rate (Webb *et al.*, 1987a; Whitehead *et al.*, 1990), incubation time (Lang and Andrews, 1994; Piña *et al.*, 2003), hatching success and sex of the hatchlings (Piña *et al.*, 2003), and survivorship and differential growth of the animals (Joanen *et al.*, 1987; Piña *et al.*, 2003, 2007).

Furthermore, for field studies and management programs, a series of morphological features should be available to relate the most relevant changes to a time scale under specific incubation conditions (Larriera A., personal communications). A classification based only on chronological age has obvious shortcomings. Exact laying time is usually unknown and variation in the development rate can occur between embryos of the same age, even within the same clutch (Donayo *et al.*, 2002). Many factors are responsible for the lack of correlation between chronological and structural age, including genetic differences in the rate development, differences in incubation temperature, gaseous and humidity fluctuations, variations in the size of individual eggs, and different developmental stages when the eggs are laid (Packard and Packard, 1984; Piña *et al.*, 2003; Webb *et al.*, 1987a). If a series of morphometric dimensions and morphological features can be correlated with the real or structural age, then we will be able to either, estimate the laying time, incubation period and prediction of hatching, or know the time an embryo should be incubated to reach a given stage. Indeed, morphometric dimension could also be used to predict the age of crocodilian embryos (Deeming and Ferguson, 1990; Platt *et al.*, 2003; Sierra *et al.*, 1996), but measuring young embryos is more difficult than the identification of their external morphology (Ferguson, 1987).

Developmental stages are defined by documenting the continuous appearance of discrete morphological char-

*Correspondence to: Pablo Siroski, Proyecto Yacaré. Av. Aristóbulo del Valle 8700, CP: 3000, Santa Fe, Argentina.
E-mail: latirostris@arnet.com.ar
Contract grant sponsor: PROYECTO YACARÉ (Min. Prod./MUPCN), Santa Fe, Argentina; Contract grant numbers: PIP # 6375 and PICT # 31679
Published online 8 August 2008 in
Wiley InterScience (www.interscience.wiley.com).
DOI: 10.1002/dvg.20413

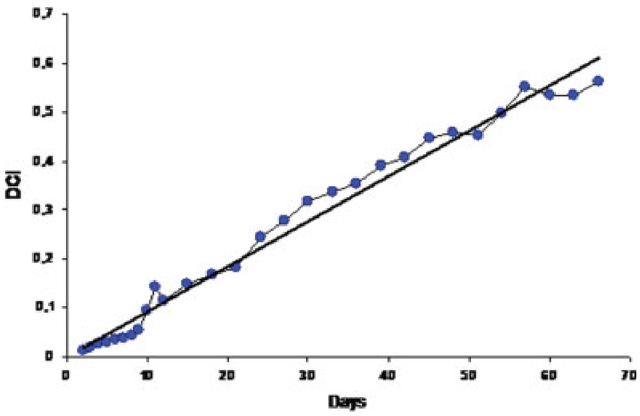

FIG. 1. Relationship between age (days) and embryo dorsal-cranial index (DCI) for *Caiman latirostris* incubated at 31°C. DCI = 0.0018 + 0.0092 days. R^2 = 98.3%. [Color figure can be viewed in the online issue, which is available at www.interscience.wiley.com.]

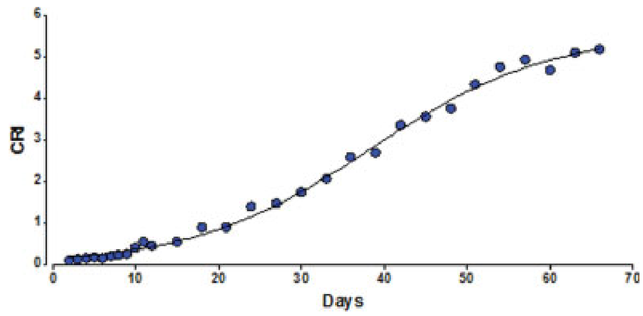

FIG. 2. Relationship between age (days) and embryo crown-rump index (CRI) for *Caiman latirostris* incubated at 31°C. CRI = $\frac{5.59}{1+35.45^{-0.09\ \text{days}}}$. [Color figure can be viewed in the online issue, which is available at www.interscience.wiley.com.]

acters. Standard morphological series have recently been published for mammals (Cretekos *et al.*, 2005), birds (Hamburger and Hamilton, 1992), and reptiles [turtles (Beggs *et al.*, 2000) and crocodiles (Hua *et al.*, 2004)]. Crocodilian embryos have been also aged on the basis of ontogenetic stages. Ferguson (1985, 1987) developed a system that divided the embryological development of crocodiles into 28 stages based on their external morphological attributes. Less comprehensive literature has also been employed to age eggs and embryos, and this information is available for *Crocodylus niloticus* (Voeltzkow, 1899); *C. porosus* (Magnusson and Taylor, 1980; Webb *et al.*, 1983a); and *C. johnstoni* (Webb *et al.*, 1983b). However, these data have little value for ageing *C. latirostris* eggs which exhibit the shortest incubation period at 29°C and one of the longest at 33°C compared to other crocodilian species (Piña *et al.*, 2003). The opaque patch is frequently used to estimate embryos age in some species. It is formed as the developing embryo takes water from pores of eggshell membrane to facilitate gas exchange. Therefore, during the incubation period, its growth is relative to the increase of embryo's size (Webb *et al.*, 1987b). Spread of opaque patch has been correlated with age in various studies (Donayo *et al.*, 2002; Joanen and McNease, 1991), though its diagnostic value is under discussion.

In this article, we establish a series of embryological descriptions for *C. latirostris*. Our study is aimed at developing a criterion for ageing embryos of *C. latirostris* using qualitative and quantitative attributes.

RESULTS

Embryo Measurements

Embryo measurements were expressed as index of egg length and plotted against their age (Figs. 1 and 2). There was a positive linear relationship between embryo age and dorsal cranial index (DCI; R^2 = 0.98), this relationship was strong up to Stage 25 (57 day), but after that residuals increased. However, the relationship between embryo age and crow rump index (CRI) was sigmoidal in nature.

Descriptions

Two-day embryo Stage 2 (E) *Figure 3a*
Extra-embryonic features.

Opaque patch covers 12% of the egg surface (see Fig. 4 for opaque patch development during incubation).
Blood-islands are present in the posterior half of blastoderm.

Cranial features.

DCL, 1 mm.
Brain vesicles. Complete fusion of neural folds. Anterior neuropore is closing. Three primary brain-vesicles are visible: forebrain, midbrain, and hindbrain, the latter appears as a transparent area.
Sensory placodes and pits. Primary optic vesicles have already formed. Auditory pits are deep and wide open.
Visceral arches. First and second visceral grooves are slightly indicated, though the arches are not yet seen.

Body.

CRL, 3.9 mm.
Flexures. The dorsal surface of the embryo is in straight line to the eggshell, and only the head is ventrally curved. Two curves are observed in the head region: cranial flexure at midbrain level and cervical flexure at heart level, where hindbrain reaches the spinal cord. Forebrain and hindbrain axes form an approximate right angle. Cervical flexure is broad and its angle is larger than 90°. Body torsion has not yet begun.
Heart. Paired cardiac primordia are fused and slightly displaced to right.

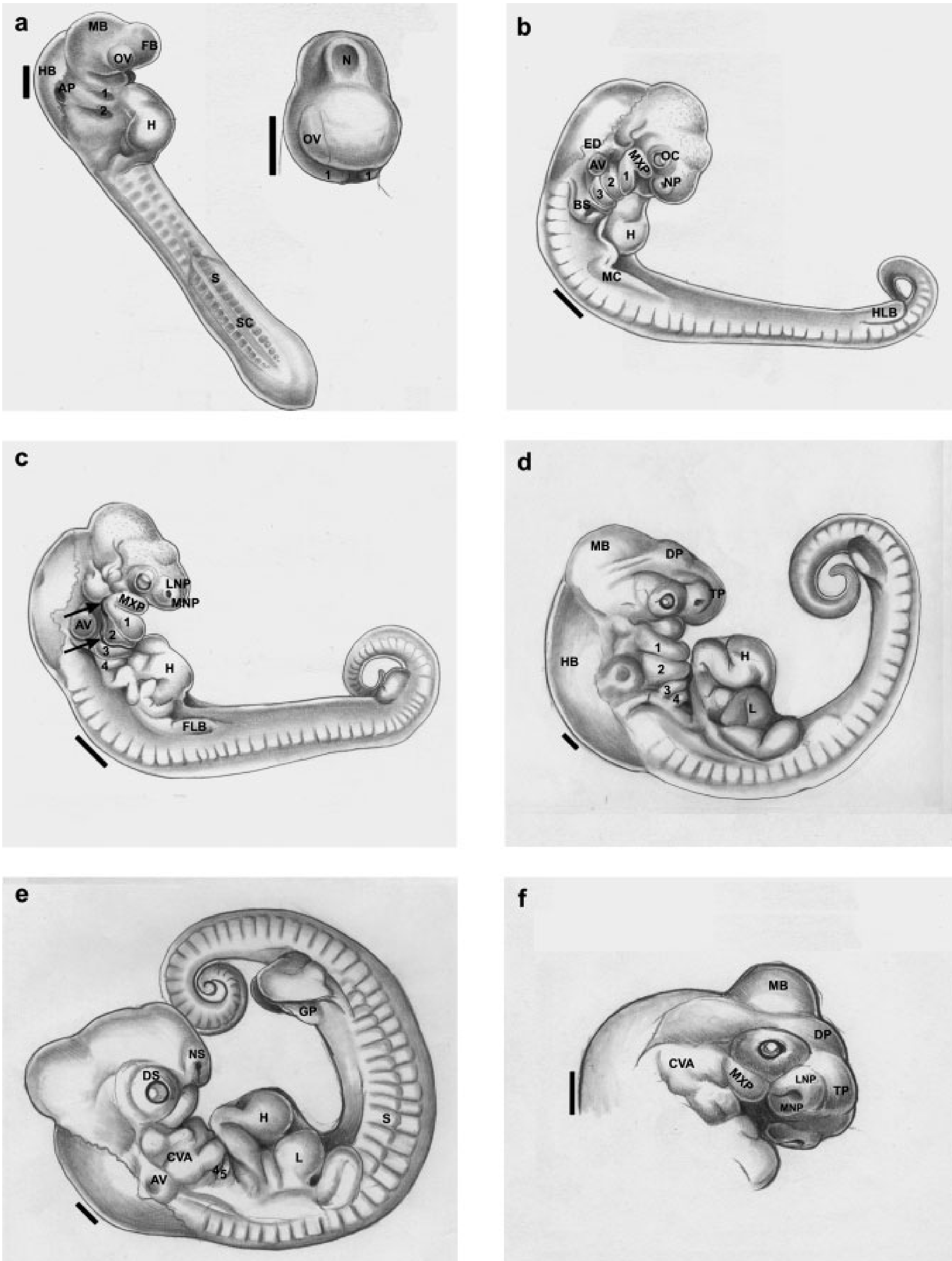

FIG. 3. *Caiman latirostris* embryos: (**a**) Day 2, left: ventral aspect, visceral grooves are numbered (1–2), right: head embryo in ventral view, note the anterior neuropore (N); (**b**) Day 7, lateral view, visceral arches are indicated 1 to 3, see Figure 5b for picture; (**c**) Day 8, lateral view, visceral arches are numbered (1–4), the arrows show visceral clefts; (**d**) Day 9, lateral view, visceral arches are indicated (1–4); (**e**) Day 11, lateral view, visceral arches 4th and 5th are indicated; (**f**) Day 12, ventral view, note how nasal slits have formed “furrows,” separating lateral from medial nasal processes. AP, auditory pit; AV, auditory vesicle; BS, branchial sinus; CVA, conglomerate visceral arches; DP, diencephalon; DS, dark stripe; ED, endolymphatic duct; FB, forebrain; FLB, forelimb-bud; GP, genital primordium; H, heart; HB, hindbrain; HLB, hindlimb-bud; MB, midbrain; MC, mesoderm condensations; MXP, maxillary process; NP, nasal pit; NS, nasal slit; L, liver; LNP, lateral nasal process; MNP, medial nasal process; OC, optic cup; OV, optic vesicle; S, somites; SC, spinal cord; TP, telencephalon. Scale bars = 0.5 mm.

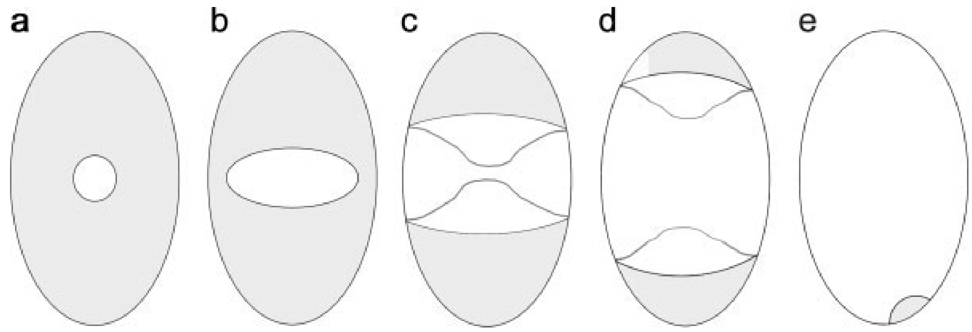

FIG. 4. Development of the opaque patch throughout incubation at 31°C. (**a**) at Day 2 the patch is just a whiter dot in the top of the egg; (**b**) at Day 3 the patch has increased in area, both in wide and length; (**c**) by Day 4 the patch have covered the minimum diameter of the egg; (**d**) approximately at Day 36 of incubation at 31°C the patch have covered about 70% of the egg; finally (**e**) by Day 57 the patch have covered almost a 100% of the egg.

Notochord and somites. The notochord runs in front of the neural tube when observed ventrally. Somite pairs (20) are present on both sides of spinal cord.

Three-day embryo Stage 3 (E)
Extra-embryonic features.

Opaque patch covers 34% of the egg surface (Fig. 4b).
Amnion and allantois are not yet formed.

Cranial features.

DCL, 1.3 mm.

Body.

CRL, 5.3 mm.
Somites, 26 pairs.
Flexures and rotation. Cranial flexure unchanged; cervical flexure is more sharply, but still larger than 90°. No body torsion.
Heart shows an S-shape and it is displaced to the left.

Four-day embryo Stage 4 (E)
Extra-embryonic features.

Opaque patch covers 35% of the egg surface and has already surrounded its minimum diameter (Fig. 4c).
Extra-embryonic membrane. Head-fold of amnion is present, extending backward to cover embryo's dorsum. The allantois appears as a small swelling on the ventral tail fold.
Blood vessels are now visible, vitelline veins emerge from the caudal limit of heart, whereas the vitelline arteries run along the lateral walls of the body sticking out at approximately the caudal third of the embryo.

Cranial features.

DCL, 1.7 mm.
Sensory placodes and *pits*. Optic vesicles begin to invaginate; lens placodes are forming from the ectoderm. The opening of auditory pits becomes narrower.
Visceral arches. First and second visceral grooves are clearly indicated.

Body.

CRL, 6.3 mm.
Somites, 32 pairs.
Flexure and rotation. Axes of forebrain and hindbrain form an acute angle. Cervical flexure is a broad curve and its angle is about right. Trunk flexure begins running backwards at heart level. The contour of the posterior part of the trunk is straight to the base of the tail. Body torsion has commenced. Head is fully turned to the right, but the caudal half has not yet rotated.
Lateral body-folds extend from the caudal heart limit to three-fourths of the body.
Heart winds itself making two pouches covered by the pericardial sac.
Tail-bud is a short cone, bent ventrally, that has three pairs of somite in its base but not in the tip.

Five-day embryo Stage 5 (L)
Extra-embryonic features.

Opaque patch covers 37% of the egg surface.
Allantois is small bulge beginning to inflate.

Cranial features.

DCL, 2.2 mm.
Pits. The opening of auditory pits is constricted.
Visceral arches, 1, 2 and 3, are outlined in the pharyngeal region.

Body.

CRL, 6.9 mm.
Somites, 36 pairs.

Rotation. The body has completely rotated to the right, except for the tail region.
Heart and blood vessels. Cardiac septa are distinct. Dorsal aorta extends from the middle of pharyngeal region toward the caudal tip of the body. Vitelline arteries are seen as lateral branches of the dorsal aorta. Blood vessels are barely distinguishable in each somite.
Tail-bud bent ventrally, contains eight somites at its base, but tip is still unsegmented.

Limbs.

Limb-primordia. Inconspicuous condensation of mesoderm is present at forelimb-level.

Six-day embryo Stage 6 (L) *Figure 5a*
Extra-embryonic features.

Opaque patch covers 39% of the egg surface.
Allantois is swollen reaching the length of the tail (see right bottom corner in the Fig. 5a).

Cranial features.

DCL, 2.5 mm.
Forebrain lengthened. Regionalization of forebrain into diencephalon and telencephalon indicated by a slight constriction.
Sensory placodes and *pits*. Lens placodes appear on primary optic vesicles. Auditory vesicles are connected to the small ectoderm opening by the endolymphatic duct. First indication of nasal pits.
Visceral arches, the 1st one is delineated.
Facial processes. Maxillary processes are slightly visible and attached to the dorsal end of the first arch.

Body.

CRL, 6.6 mm.
Flexures and rotation. At the cervical flexure, the axis of the medulla forms approximately a right angle to the axis of the posterior trunk. Trunk flexure shifts to the posterior part of the body, but the contour of mid-trunk is still straight. The body is completely rotated.
Tail-bud is curved and its tip pointing forward.

Limbs.

Limb-primordia: Inconspicuous condensation of mesoderm at hindlimb-level.

Seven-day embryo Stage 7 (L) *Figures 3b and 5b*
Extra-embryonic features.

Opaque patch covers 43% of the egg surface.
Allantois is now higher than the tail but not fused with the chorion yet, on its surface, blood vessels appear.

Cranial features.

DCL, 2.6 mm.
Five brain vesicles are present, constriction between forebrain-parts has deepened, but regionalization of hindbrain is indicated by a slight constriction.
Sensory placodes and *pits*. Optic cups are formed by a double contour broken by the choroid fissure. The auditory vesicle loses its spherical shape as endolymphatic duct develops dorsally, which can be seen now through the neural epithelial tissue. Nasal pits are formed.
Facial processes. Maxillary processes extend under eye as far as its middle but they are still shorter than the mandibular arch. Medial and lateral nasal processes appear as distinct elevations on both sides of nasal pits.
Three visceral arches project over the surface. The 1st and 2nd visceral grooves are cleft, but they are only present on the dorsal third of the 1st groove and the dorsal half of the 2nd. The branchial sinus is found in the caudal tip of the 3rd arch.

Body.

CRL, 8.4 mm.
Flexures. The cranial flexure makes the nasal region point toward the heart forming an acute angle. In the cervical flexure, the axis of the medulla forms an acute angle with the trunk axis.
Tail. The tip of the tail is curved at approximately 90°.

Limbs.

Hindlimb-bud is a thickened ridge, but primordium of forelimbs is still flat.

Eight-day embryo Stage 8 (L) *Figure 3c*
Extra-embryonic features.

Opaque patch covers 46% of the egg surface.
Allantois and chorion fused.

Cranial features.

DCL, 2.9 mm.
Optic cups unpigmented.
Four visceral arches are evident. The 1st visceral cleft is dorsally located, which is immediately ventral to the otocyst.

Body.

CRL, 9.7 mm.
Flexure. Cranial flexure is unchanged. The bend in

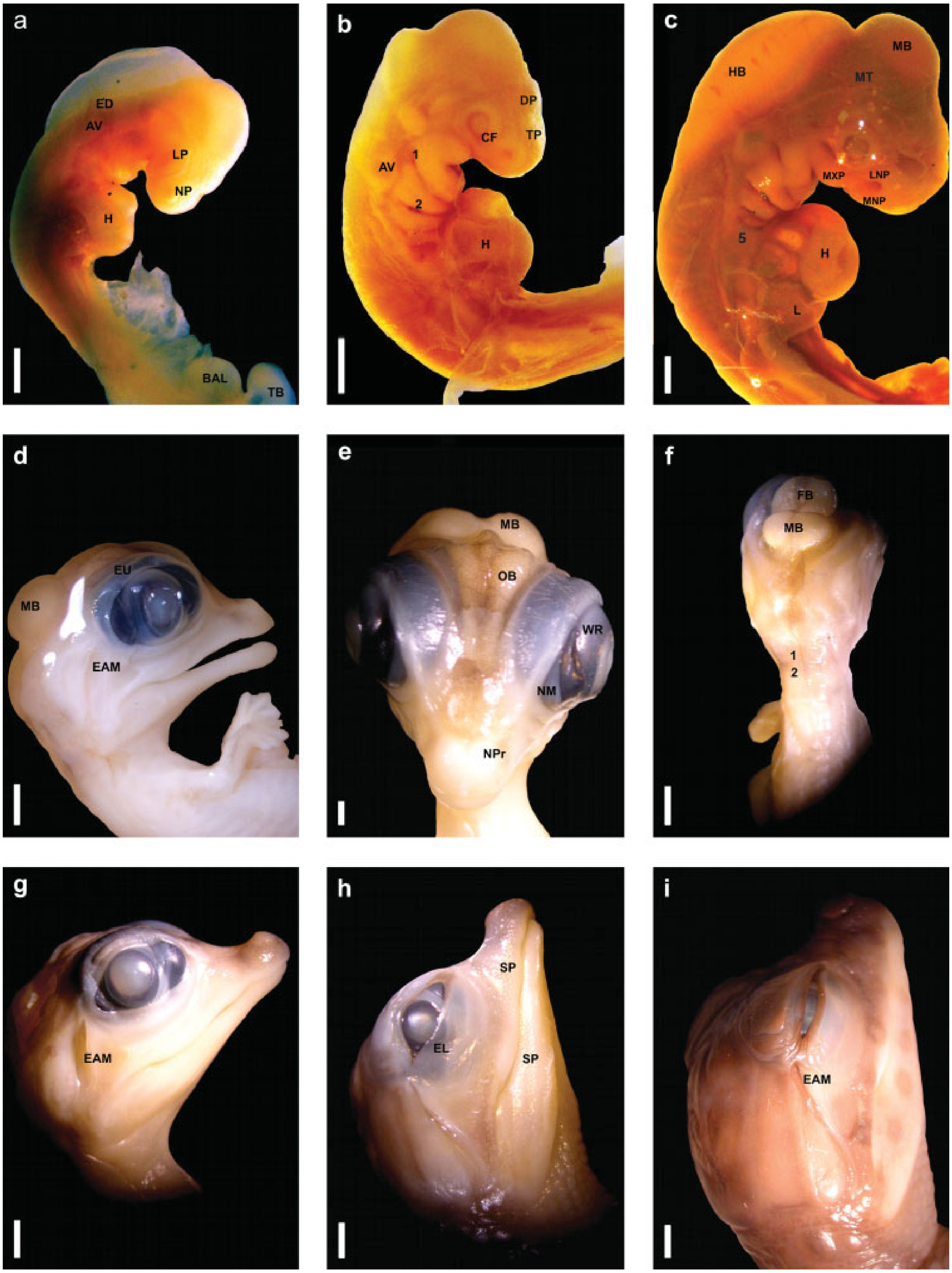

FIG. 5. *Caiman latirostris* embryos: (**a**) Day 6, lateral view; (**b**) Day 7, lateral view, numbers (1–2) indicate visceral clefts, see Figure 3b for drawing; (**c**) Day 10, lateral view, 5th visceral arch is indicated; (**d**) Day 24, lateral view, observe the curvature of the upper jaw, see Figure 7d for drawing; (**e**) Day 24, frontal view, the white ring (WR), see Figure 7d for drawing; (**f**) Day 27, dorsal view, scutes are numerate in rows 1 and 2; (**g**) Day 30, lateral view; (**h**) Day 36, lateral view; (**i**) Day 42, note spotted aspect pattern of the jaws. AV, auditory vesicle; BAL, but allantois; CF, choroid fissure; DP, diencephalon; EAM, external auditory meatus; ED, endolymphatic duct; EL, lower eyelid; EU, upper eyelid; FB, forebrain; H, heart; HB, mielencephalon; L, liver; LNP, lateral nasal process; LP, lens placode; MB, midbrain; MNP, medial nasal process; MT, metencephalon; MXP, maxillary process; NM, nictitating membrane; NP, nasal placode; NPr, nasal processes; OB, olfactory bulbs; SP, sensory papillae; TB, tail bud; TP, telencephalon. Scale bars from a–c represent 0.5 mm and from d–i represent 2 mm.

the tail-region begins to extend forward into lumbo-sacral level.
Genital primordium is a small elevation.

Limbs.

Forelimb-bud is a thickened ridge. The apical ectodermal ridge is developing on the hindlimb bud.

Nine-day embryo Stage 9 (L) *Figure 3d and 6a*
Extra-embryonic features.

Opaque patch covers 40% of the egg surface.

Cranial features.

DCL, 3.7 mm.
Optic cups pigmentation is a faint greyish hue. Choroidal fissure is no longer visible.
Maxillary processes extend forward beyond the eye, being shorter than the mandibular arch though.
Visceral arches. The 2nd arch has broadened, overlapping the 3rd one. Mandibular arch is lobulated in the middle when ventrally viewed.

Body.

CRL, 10.6 mm.
Trunk-flexure is distinct at the lumbo-sacral and thoracic level, so the dorsal hindbrain-tail contour is a curved line.
Guts. The liver is an asymmetric bulge lying under the heart.
Tail is curled through three 90° turns.

Limbs.

Limb-buds are wider in the base than higher. The apical ectodermal ridge is present on both buds.

Ten-day embryo Stage 10 (E) *Figures 5c*
Extra-embryonic features.

Opaque patch covers 41% of the egg surface.

Cranial features.

DCL, 6.3 mm.
Brain vesicles. No constriction is present clearly between hindbrain-parts, though the latter can be distinguished for its thin transparent wall.
Nasal slits lengthened extending towards the primitive oronasal cavity.
Maxillary processes are continuous with the lateral nasal processes.
Five visceral arches present the 1st and 2nd being the largest and the 5th the smallest.

Body.

CRL, 17.2 mm.

Limbs.

Limb-buds. Both are distinct swellings of approximately equal size.

Eleven-day embryo Stage 12 (E) *Figure 3e*
Extra-embryonic features.

Opaque patch covers 41% of the egg surface.

Cranial features.

DCL, 8.1 mm.
Eyes pigmentation is a distinct dark black in the iris.
Visceral arches, the 3rd arch is overgrown by the 2nd arch, whereas the 4th and 5th arches are markedly reduced.
Maxillary and lateral nasal processes are fused, mandibular process is present but inconspicuous.

Body.

CRL, 20.5 mm.
Somites are segmented by half, bending into an obtuse angle to the cranial apex.
Genital primordium reaches the height of the limbs.
Tail is distinctly coiled at caudal tip.

Limbs.

Limb-buds lengthened, now being longer than wider and pointing to the caudal tip of the body.

Twelve-day embryo Stage 12 *Figure 3f*
Extra-embryonic features.

Opaque patch covers 42% of the egg surface.

Cranial features.

DCL, 7 mm.
Eyes. The optic cups and central lens are large and round eyeballs.
Nasal slits have already reached the roof of oronasal cavity separating medial from lateral nasal processes.
Visceral arches. The 3rd, 4^{th}, and 5th arches are completely overgrown by the 2nd arch, forming a conglomerate on their dorsal aspect.

Body.

CRL, 17.5 mm.
Trunk-flexure. The embryo is completely flexed with the head touching the tail tip.

Fifteen-day embryo Stage 15 *Figures 6b, 7a,b*
Extra-embryonic features.

Opaque patch covers 45% of the egg surface.

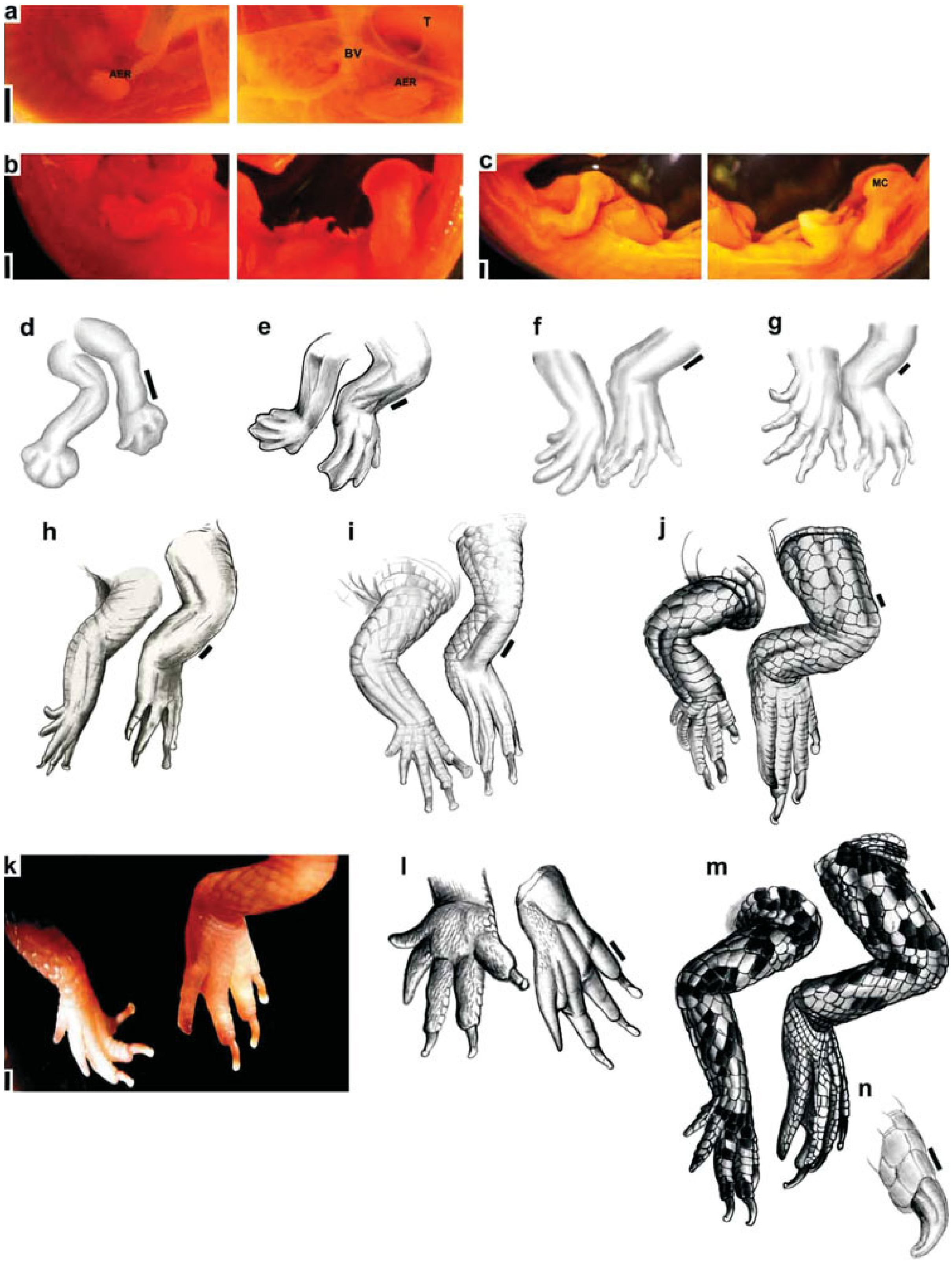

FIG. 6. Right forelimbs and hindlimbs of *Caiman latirostris* embryos. All pictures are dorsal apect, except for pictures (**l**) and (**n**). (**a**) Day 9, projection of bud limbs from the flank, note the apical ectodermal ridge; (**b**) Day 15, note the bents of the elbow-joint and knee-joint; (**c**) Day 18, observe the mesodermal condensations (MC); (**d**) Day 21; (**e**) Day 24; (**f**) Day 27; (**g**) Day 30; (**h**) Day 33; (**i**) Day 36; (**j**) Day 39; (**k**) Day 42; (**l**) Day 51, ventral aspect palm and sole surface showing the scales; (**m**) Day 54; (n) Day 66, claws from lateral view, note the groove extending on its surface. In Day 15 (b) distal and proximal elements are already differentiated. Up to Day 27 (f) no structure, except for mesodermal condensation, is visible macroscopically at limb-level, later digital differentiations, nails appear, and scales process occur. AER, apical ectodermal ridge; BV, blood vessels extra-embryonic; T, tail. Scale bars from (a) represent 0.25 mm; from (b–g) represent 0.5 mm; from (h–l) represent 1 mm; and from (m–n) represent 2 mm.

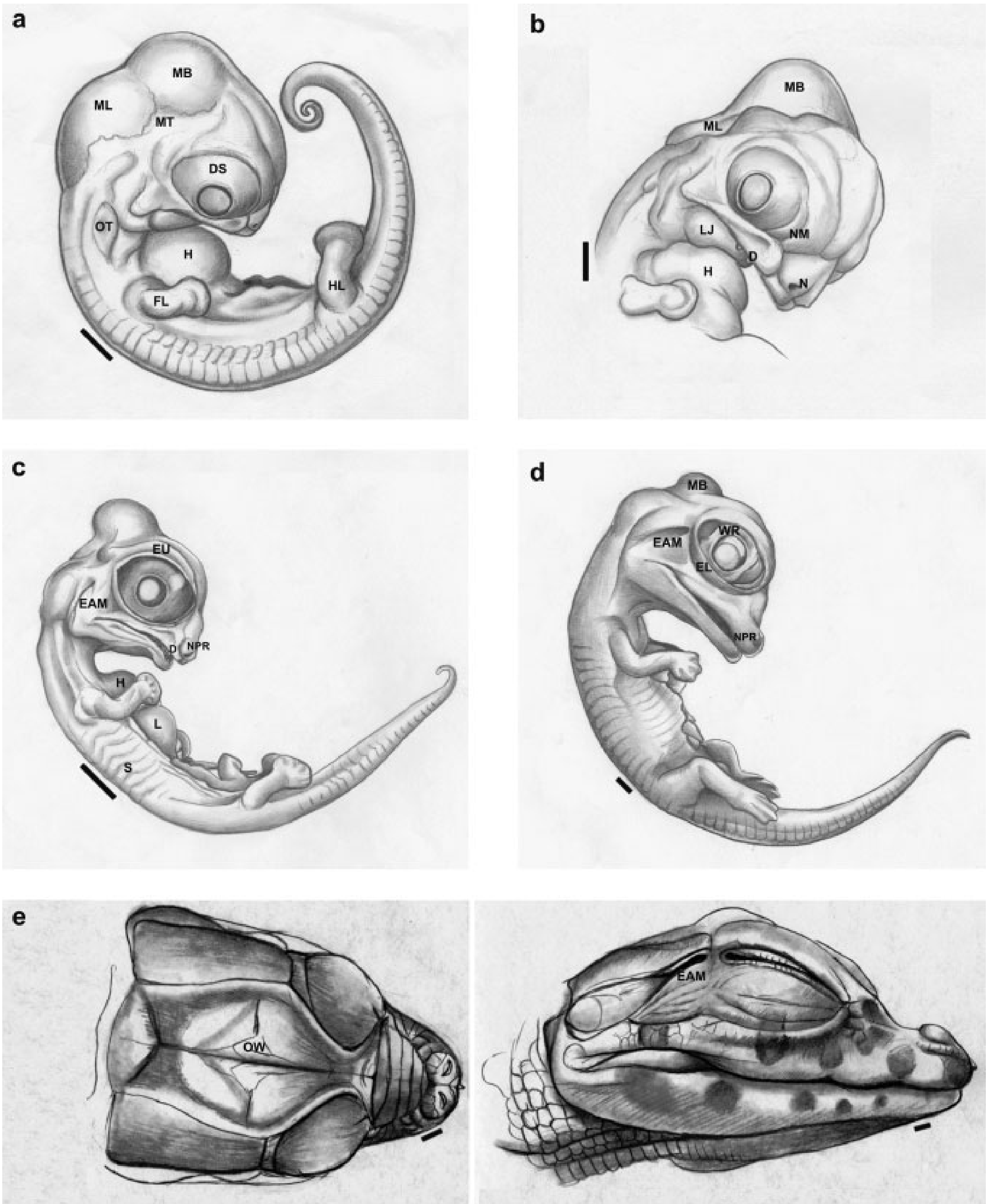

FIG. 7. *Caiman latirostris* embryos: (**a**) Days 15, lateral view, (**b**) head from ventral view; (**c**) Day 18, lateral view; (**d**) Day 24, lateral view, see Figure 5d,e for pictures; (**e**) embryo head on Day 48, left: dorsal aspect (see the oval window-OW), right: lateral view. D, denticle; DS, dark stripe; EAM, external auditory meatus; EL, lower eyelid; EU, upper eyelid; FL, forelimb; H, heart; HL, hindlimb; L, liver; LJ, lower jaw; MB, midbrain; ML, mielencephalon; MT, metencephalon; N, nostril; NM, nictitating membrane; NPR, nasal process; OT, otocyst; S, somites; WR, white ring. Scale bars = 1 mm.

Cranial features.

DCL, 9.3 mm.
Hindbrain is smaller (have become shorter and thinner) in relation to the head, and its walls are now thicker.
Eyes. Protruding eyeballs. Nictitating membrane has developed in the anterior corner of the eyes.
Otocyst lengthened. Endolymphatic duct is no longer visible.
Nasal slits are now rounded pits.

Visceral arches are not visible. The 1st visceral cleft is sinusoidal in outline, situated above the otocyst.
Facial processes. Maxillary processes extend forming a continuing base beneath the eyes and the medial and lateral nasal processes. Lower jaw extends beneath maxillary processes up to the middle eyes level.
Denticles. Two denticles are present on both sides of the anterior margins of upper jaw.

Body.

CRL, 21.2 mm.
Trunk-flexure is less bent and head no longer touching the tail tip. The face lies against the heart.
Heart is less prominent. Abdominal walls have grown but ventricles and liver and other organs are still visible.

Limbs.

The main segments of the limbs are demarked. Limbs are slightly flexed at the elbow-joint and knee-joint levels. Digital plate is present but still smooth.

Eighteen-day Embryo Stage 17 (L) and 18 (E) *Figures 6c and 7c*
Extra-embryonic features.

Opaque patch covers 43% of the egg surface.

Cranial features.

Jaw and neck have elongated conspicuously.
DCL, 10.6 mm; *EYL*, 3.1 mm.
Hindbrain is not visible while midbrain forms a prominent bulge. The olfactory bulbs are clearly distinct.
Eyelids have developed on the upper edge of the iris.
Auditory cleft. The 1st visceral cleft is now more horizontally oriented and is hereafter called the external auditory meatus. A groove runs craniocaudally along basal aspect of the lower jaw.
Nasal processes project, forming two antero-dorsal bulges.
Jaw is slightly hook-shaped. Lower jaw extends almost to the end of the upper jaw.
Denticles. Five denticles are present on the upper jaw and four on the lower jaw.

Body.

CRL, 35.5 mm.
Flexure. Cervical flexure straightens; the head no longer lies on the heart. Body flexure is less bent than in the previous days.
Heart sited in thoracic region.
Somites are zigzag-shaped.
Guts. Mesonephros are ventrally outlined.
External genitalia primordium has lengthened.

Limbs.

Faint demarcation of five fingers and four toes. Limbs sharply flexed.

Twenty one-day embryo Stage 18 *Figure 6d*
Extra-embryonic features.

Opaque patch covers 38% of the egg surface.

Cranial features.

The lengthening of neck and jaws continues. Eyeballs and jaws have enlarged, constituting most of skull space.
DCL, 12.1 mm; *EYL*, 3.8 mm.
Eyelid development is visible and with upper and lower lids gently touching.
Jaws are markedly hook-shaped.

Body.

CRL, 34.5 mm.
Circulatory system. Thoracic walls begin to cover the heart. More blood vessels are observed at the midbrain and limb-level, but not in the distal elements.

Limbs.

Sharp demarcation of fingers and toes. The periphery of the digital plate is slightly serrated.

Pigmentation and other features.

Pigmentation. White flecks representing underlying ossification are visible on the margins of the jaws.

Twenty four-day embryo Stage 19 *Figures 5d,e, 6e, and 7d*
Extra-embryonic features.

Opaque patch covers 34% of the egg surface.

Cranial features.

Eyes and jaws are now smaller in relation to the head.
DCL, 15.4 mm; *EYL*, 5.1 mm.
Midbrain development outlines a square head.
Eyes. Upper and lower lids meet encompassing the eye, but lids are narrower in the joining point than in the rest of the eyelid. Nictitating membrane remains extended. White ring in the iris surrounds the outer edge of the lens.
Nasal processes have coalesced at the middle line displacing nostrils dorsally.
Jaws are straight now. Lower jaw extends just behind the upper jaw end.

Body.

No longer out of proportion with head.
CRL, 54.7 mm.
Heart is progressively covered by thoracic walls.
Ribs are noticeable through the ventral walls.
External genitalia primordium is now pointed with a distinct elevation in its tip.

Limbs.

Digital ridges are convex due to interdigital web apoptosis.

Pigmentation and other features.

Pigmentation. White flecks are present along jaw margins, around the external auditory meatus, under the eyes, and in the posterior edge of the skull. Faint pigmentation is seen in the dorsal aspect of the snout, the skull, and limbs.

Twenty seven-day embryo Stage 20 (L) *Figures 5f and 6f.* The embryo commences to show some taxonomical features such as nuchal scutes.
Extra-embryonic features.

Opaque patch covers 40% of the egg surface.

Cranial features.

Snout has elongated, relative to the rest of the head.
DCL, 17.6 mm; *EYL*, 4.6 mm.
Midbrain appears as a tiny bulge, giving head a semicircular shape.
Eyelids outline an oval circumference reaching of eye white ring.
Nostrils are elevated on nasal discs.
Jaws are fully formed.

Body.

CRL, 57.5 mm; *SVL*, 28.1 mm.
Circulatory system. Vessels emerge from the umbilical stalk. One pair encompasses the yolk sac, whereas the other pair extends toward the allantois.

Limbs.

Phalanges become apparent in the digits. Convexity of digital ridges is at highest point reaching its adult-level. Differences in size of individual digits are conspicuous.
Nail anlagen develop on 1st, 2nd, and 3rd toes, but their formation is not clear on the fingers.

Pigmentation and other features.

Sensory papillae appear as faint elevations on jaw margins.
Scales are evident along both ventral and dorsal surface of the body and around the tail.
Scutes appear in the back neck region.

Thirtieth-day embryo Stage 21 (L) *Figures 5g and 6g*
Extra-embryonic features.

Opaque patch covers 51% of the egg surface.

Cranial features.

DCL, 20 mm; *EYL*, 5 mm.
Brain lobes are still visible but the top of skull has almost closed posteriorly.
Nictitating membrane has grown conspicuously reaching the lens of the eyes.

Body.

CRL, 66.4 mm; *SVL*, 34.3 mm.
Heart is nearly covered by thoracic walls, and abdominal guts are no longer visible.

Limbs.

Phalanges. A series of bulges in the digits mark the beginning of the interdigital joints.
Nail anlagen develops on 1st, 2nd, and 3rd fingers.

Pigmentation and other features.

Pigmentation is visible in the upper jaw margins and extends dorsally. Pigmented large scales on the back give the embryo a finely mottled brown appearance.

Thirty third-day embryo Stage 22 *Figure 6h*
Extra-embryonic features.

Opaque patch covers 51% of the egg surface.

Cranial features.

DCL, 21.3 mm; *EYL*, 4.9 mm.
Eyelid width is uniform. Lower eyelid reaches the level of the lens.
Auditory meatus is mere a cleft laying immediately after the dorsal limit of the eyes. It is overgrown by ear flap.

Body.

RCL, 78.2 mm; *SVL*, 39.6 mm.
Heart is completely covered by lateral walls which have already closed.
External genitalia primordium is prominent and the lips of the cloaca start to develop.

Limbs.

Nails are distinct on both fingers and toes, and their tips are slightly curved and enclosed in "sheaths."

Pigmentation and other features.

Scales are present on flanks and neck fusing at the ventral part of the jaws.

Thirty sixth-day embryo Stage 23 *Figures 5h and 6i*
Extra-embryonic features.

Opaque patch covers 73% of the egg surface (Fig. 4d).

Cranial features.

DCL, 22.3 mm; *EYL*, 5.2 mm.
Brain: in a lateral view, it is at a same level than skull.
Lower eyelid crosses the lower margin of the lens. Opening between lids much reduced.

Body.

CRL, 98.2 mm; *SVL*, 47.2 mm.

Limbs.

Claws of toes and fingers are flattened laterally and curved ventrally; dorsal tips are opaque, indicating onset of cornification.

Pigmentation and other features.

Sensory papillae are now seen as distinct swellings that run along the jaw margins.
Scales spread throughout the surface of the limbs, being still faint in their dorsal aspect.
Pigmentation has extended toward the dorsal aspects of the flanks, tail tip, and all elements of the limbs.

Thirty nineith-day embryo Stage 23 (L) *Figure 6j*
Extra-embryonic features.

Opaque patch covers 81% of the egg surface.

Cranial features.

DCL, 24.7 mm; *EYL*, 6.2 mm.
Lower eyelid covers less than half of the pupil.
Egg tooth has appeared in the tip of the snout lying against a smooth and white surface.

Body.

CRL, 105 mm; *SVL*, 54.2 mm.
External genitalia primordium reaches the height of cloaca lips.

Limbs.

Claw formation is complete and the hooking becomes more marked toward hatching. A groove runs along the external surface of the claws.

Pigmentation and other features.

Nuchal Scutes are established, showing an adult pattern.
Pigmentation has increased, giving the animal a light brown color, but the ventral aspects are still unpigmented or pale. Dorsal stripes are present. The ventral part of jaws and neck are reddish, which indicates significant development of blood vessel plexus.

Forty second-day embryo Stage 24 *Figures 5i and 6k*
Extra-embryonic features.

Opaque patch covers 86% of the egg surface.

Cranial features.

DCL, 26.5 mm; *EYL*, 6.6 mm.
Skull is strongly ossified, but brain is still obvious through its top.
Eyelids. Upper lid tissue has scutes and is pigmented. Lower lid covers more than half of the pupil, but the eyelids are not able to fully close. Opening between eyelids reduced to a thin crescent.

Body.

CRL, 124 mm; *SVL*, 60.9 mm.

Pigmentation and other features.

*Scale*s are now evident throughout embryo surface. Double row of raised scutes along the proximal portion of the tail is obvious but not as sharply marked as the single row of raised scutes of its distal end.
Pigmentation is stronger so the embryo is now dark brown, and jaws are spotted.

Forty fifth-day embryo Stage 24. Few macroscopic changes are evident at this and later days.
Extra-embryonic features.

Opaque patch covers 89% of the egg surface.

Cranial features.

DCL, 28.2 mm; *EYL*, 6.5 mm.
Eyelids are fully formed and able to close. *Eyelid* opening has been reduced to narrow slit.

Body.

CRL, 139 mm; *SVL*, 66.8 mm.
External genitalia primordium is no longer visible.

Forty eighth-day embryo Stage 24 *Figure 7e*
Extra-embryonic features.

Opaque patch covers 85% of the egg surface.

Cranial features.

DCL, 29.7 mm; *EYL*, 7 mm.
Skull ossification appears virtually complete except for a small oval window in the dorsal center of skull platform through which the brain could be seen.

Body.

CRL, 143 mm; *SVL*, 68.2 mm.

Pigmentation and other features.

Scales. Upper jaw covered by well-formed scales.

Fifty first-day embryo Stage 24 *Figure 6l*
Extra-embryonic features.

Opaque patch covers 82% of the egg surface.

Cranial features.

DCL, 30.4 mm; *EYL*, 7.1 mm.
Preocular ridges appear, but become more prominent later in the development.

Body.

CRL, 165 mm; *SVL*, 78.1 mm.
*Scale*s are hardly crested and distinctly marked along the dorsal surface. Lower jaw, palm, and sole surface are covered by well-formed scales.

Pigmentation and other features.

Pigmentation has become greenish-black, but still faint ventrally.

Fifty fourth-day embryo Stage 25 *Figure 6m*
Extra-embryonic features.

Opaque patch covers 91% of the egg surface.

Cranial features.

DCL, 31.8 mm; *EYL*, 7.2 mm.
Brain is completely enclosed by bone.
Musk glands are slightly visible along the posterior lateral margins of the intergular floor of the lower jaw.

Body.

CRL, 181 mm; *SVL*, 82.7 mm.

Limbs.

Claws are well-hooked.

Pigmentation and other features.

Pigmentation. Flanks and cranial skin become spotted.

Fifty seventh-day embryo Stage 25. Eggshell has become completely opaque (Fig. 4e). The embryo looks like a small hatchling with a considerable amount of external yolk attached to its umbilical region.

Cranial features.

DCL, 33.6 mm; *EYL*, 6.9 mm.

Body.

CRL, 192 mm; *SVL*, 88.3 mm.

Sixtieth–sixty third-day embryo Stage 27. Opaque patch coverage is complete. Since this stage, embryonic measurements show little variation and are not further presented. These days are characterized by the withdrawal of the remaining yolk. This process ends when the yolk is completely withdrawn into the body cavity, leaving the yolk scar.

Sixty sixth-day embryo Stage 28 *Figure 6n.* Opaque patch coverage is complete. The yolk scar diminishes in length and width as the withdrawn abdominal yolk is absorbed. There are considerable variations in the volume of absorbed yolk and the size of the yolk scar at hatching.

DISCUSSION

In a landmark study, Ferguson (1985, 1987) developed a staging scheme for ageing crocodile embryos, applying such scheme in three species from two families. Few further studies have made use of qualitative attributes to determine the age of embryos (Hua *et al.*, 2004). Instead, they have focused on quantitative attributes alone, like spread of opaque patch (Donayo *et al.*, 2002; Joanen and McNease, 1991) and embryo measurements (Deeming and Ferguson, 1990; Platt *et al.*, 2003; Sierra *et al.*, 1996). The present study demonstrates the value of both qualitative and quantitative attributes for determining the age of *C. latirostris* embryos. The opaque patch extent pattern found in our research coincides with some previous studies in *C. latirostris* (Donayo *et al.*, 2002); and in other crocodiles (Ramírez-Perilla, 2005; Webb *et al.*, 1987b). As described by Donayo *et al.* (2002), ageing 0–4 days embryos is possible using the banding method, but in intermediate period (5–36 days, Stages 5–22), the patch shows great variability (see Days 15 and 27 as example). In addition, as stated by Larriera *et al.* (1996), there is no clear-cut distinction of patch edges in the late stages. Therefore, the spread of patch yielded little reliable information for ageing intermediate and later incubation if compared with embryo descriptions. Nevertheless, direct embryo measurements proved to be a reliable method for ageing. There were close relationship between age/stage and the CRI up to Stage 26, after which CRI was relatively constant; confirming Webb *et al.* (1986) observations that in *Carettochelys insculpta*, embryo size reaches a maximum before qualitative changes are complete. Other studies (Deeming and Ferguson, 1990; Platt *et al.*, 2003) have identified DCL as the best attribute to predict embryonic age in crocodilians. We found a significant positive relationship between embryos age and DCL, but this measurement was associated to great errors when ageing younger embryos (Stage 2–18). Despite the fact that embryo growth had slowed at Stage 26, some other quantifiable features may have varied up to hatching (Stage 28). However, all measurements collected here remained constant after Stage 26.

We were able to distinguish 28 stages on the basis of morphologic attributes alone. There were three main periods during the development in which morphologic attributes were useful. Ageing in early stages (2–12 day, Stages 2–12) could be determined by observing primary brain vesicles, sensory placodes, visceral arches, flexure and rotation, and number of somites; and in intermediate stages (15–39 day, Stages 15–23) by limb morphology and craniofacial features; whereas in later stages (39–51 day, Stages 23 and 24) pigmentation and scales pattern are the most outstanding attributes. Beyond Stage 5 the number of somites became increasingly difficult to determine with accuracy. This is due, in part, to the dispersal of the mesoderm of the anterior-most somites, and in later stages, to the curvature of the tail. For these reasons, other external structures were used as identifying criteria from Stage 5 onward. We can state that up to Stage 21, external morphologic features, which are easy to identify, are accurate age predictors, due to fast development, shorter stages intervals, and the difficulty to measure young embryos. However, for older embryos, morphological attributes, together with morphometric ratios, must be considered to age embryos accurately (these observations were also made by Ferguson, 1987). Consequently, the application of measurements/stage relationship to ageing is limited to the period of development up to Stage 26, then—before hatchling—the proportion of yolk internalization could be consider as an ageing indicator.

Any staging system imposes a set of convenient, but arbitrary, standards for a conceptual division of what in reality is a continuous process of change over time. In this research, there were some occasions in which we were not able to assess accurately whether a specimen was older for a given stage or younger for the subsequent one (as described by Ferguson, 1987). We have endeavored to minimize such ambiguity by making use of the letter (E) to indicate an early embryo and (L) for a later embryo in a particular stage compared with those of Ferguson (1987). For example in this series, Days 8 and 9 have an (L) since the embryos have four visceral arches in these days and not three as it has been described in Ferguson's staging system (1985, 1987). It was also difficult to deal with embryos which presented characteristics of more than one stage (an 18-day embryo appears either in Stage 17 or Stage 18). As it was expected, late stages took more than 3 days and therefore, many developed embryos (42–51 and 54–57 days) share the same embryologic stage (24–25, respectively; Andrews and Mathies, 2000; this work).

The approach of this work was to calibrate our results against Ferguson's standard series (1985, 1987). We can claim that *C. latirostris* embryonic development fits such a series, nevertheless some differences were found (see Table 1). For instance, according to Ferguson's series, visceral arches appear before Stage 7, but in our research those arches are distinctively visible only at Stage 7. It could be said that the two grooves observed from Days 2–4 indicated visceral segments that will be the visceral arches later in development, but these are not distinct enough to be called arch. Furthermore, in our work, as well as in some other studies with turtles, birds, and bats (Beggs *et al.*, 2000; Cretekos *et al.*, 2005; Hamburger and Hamilton, 1992), the previous or simultaneous appearance of forelimb buds, with regards to hindlimb buds, does not correspond with Ferguson's description. However, the rapid development of the hindlimbs may justify what Ferguson (1985, 1987) stated. Scale and pigmentation patterns also show differences in late stages. In contrast to other crocodiles, *C. latirostris* scales appear once jaws and nails are fully formed (Ferguson, 1987). In our study, pigmentation begins along the dorsal aspect of head-trunk and in the proximal and distal elements of the limbs. Then it extends on the ventral aspects of the flanks, but there is little or no pigmentation ventrally, which is different from other crocodiles in which pigmentation appears first on the ventral aspects and extends dorsally (see Ferguson, 1985, 1987).

We suspect that these differences may be due to two reasons. First, there is no standardized definition of the development of specific structures, such as when mesoderm pharyngeal grooves could be called an arch. Second, there is probably a problem with the timing of observation in Ferguson's (1985, 1987) studies for the detection of hind limb buds. We believe that the development of crocodilian hindlimb buds, although initiated after the forelimbs, rapidly outgrow them due to the importance in functionality of these hindlimbs. In all extant crocodilian species, and also in the ancestral forms, the legs are more important in function and size than forelimbs. There was even speculation that the ancient croc-

Table 1
Detailed List of Specific Characteristics for Ageing Caiman latirostris Embryos That Match, and Those That Do Not Match Ferguson (1985, 1987) Stages

Age (days)	Ferguson stages	Features do not match ferguson stages	Features match ferguson stages
2	2 (E)	**Three primary brain vesicles**. Primary optic vesicles are not invaginated, and lens placodes are not formed yet. Visceral arches are not noticeable, visceral cleft absent.	**Optic and auditory placodes are present**. **Twenty pairs of somites**. Cranial and cervical flexure indicated. Paired primordia of heart fused.
3	3 (E)	Amnion absent. Heart S-shaped, bent to right. Tail bud absent.	**Twenty six pairs of somites**.
4	4 (E)	Optic vesicles are invaginating, lens placodes are forming. **Tail bud forms and bent**.	Head fold of amnion present. **Allantois bud formed. Thirty two pairs of somites. Head turned to the right**.
5	5 (L)	**Forelimb-primordia present**.	**Thirty six pairs of somites**.
6	6 (L)	Auditory pits still open, endolymphatic duct present. **Maxillary processes are distinct**.	Lens placodes are formed. Telencephalon indicated. **Indication of nasal placodes. Embryo rotation is completed. Hindlimb-primordia present**. Tail-bud curved.
7	7 (L)	**Nasal placodes are distinct pits**, nasal processes are conspicuous.	**Optic cups complete**, choroid fissure visible. Auditory pits closed. **Three visceral arches, two grooves, two clefts and** branchial sinus are present. **Distinct hindlimb-bud**.
8	8 (L)	Allantois and chorion fused. **Four visceral arches**.	**Distinct forelimb-bud**. AER is preset on hindlimb-buds. Genital primordial appears.
9	9 (L)	**Eyes pigmented** in the iris. AER is present on forelimb-buds.	Liver is visible.
10	10 (E)	**Limb-buds symmetrical**, digital plate absent.	**Five visceral arches are present**.
11	12 (E)	Not constriction for proximal and distal elements is marked in the limbs.	Retina is dark grey. **Visceral arches are reduced**. Maxillary and lateral nasal processes are fused, mandibular process is inconspicuous. **Limbs enlarged**.
12	12		**Trunk flexure well developed**.
15	15	Eyelids development: nictitating membrane is present.	**Visceral arches are not visible. Lower jaw conspicuous. Hand plate and footplate form,** but smooth. Trunk-flexure less bent.
18	17 (L)–18 (E)	**Lower jaw extends to the end of the upper jaw**. Scales are absent.[a]	Upper eyelids development. **Jaw is hook-shaped. Cervical flexure straightens. Limbs digital condensations**.
21	18		Lower eyelids development. **Limbs interdigit tissue receding**.
24	19	**Lower jaw is straight**.	Upper and lower lids are distinct.
27	20 (L)	**Interdigital tissue disappears,** fingers and toes get lengthened. Sensory papillae are present.	**Jaw formed**. **Nail anlagen on 1st, 2nd and 3rd toes,** but not on fingers. **Scales evident on dorsal and ventral aspect, nuchal scutes beginning to appear**.
30	21 (L)	**First indication of pigmentation**. [a] Nuchal scutes are not established.	Circumference of eyelids oval. **Nail anlagen are now present on 1st, 2nd and 3rd fingers**.
33	22 (L)	Eyelids are not able to close. **Heart is not longer visible. Claws are enclosed in "sheaths," curved** and pigmented. Sensory papillae clearly evident.	Scales absent on the proximal and distal elements of the limbs. Pigmentation is still faint.
36–39	23 (L)	**Lower eyelid covers less than half of the pupil**. Claws formation is complete.	**Pigmentation more extensive, but embryos are a light brown color**. Scales present on the elements of the limbs, nuchal scutes established.
42–51	24	Midbrain is not enclosed by bone.	**Eyelids are able to close. Embryos are a dark brown color**.
54–57	25		**Brain is completely enclosed by bone**. Musk glands visible.
	26	This stage does not occur in *Caiman latirostris*, which is characterized by eruption of egg teeth.	
60–63	27		Withdrawal of remaining yolk into abdominal cavity.
66	28		Yolk scar diminishing.

AER, apical ectodermal ridge. Bolds represent features of *C. latirostris* embryos that are useful for ageing embryos.
[a]Represents specific characteristics.

odilian forms were bipeds (Colbert and Mook, 1951). However, in avian and bats, the forelimbs also appear first (maybe phylogenetic inertia), followed by the hindlimbs, and then continue to outgrow the hindlimbs due the important functionality of the forelimbs in flight. On the other hand, later appearance of scales and pigmentation pattern are unique characteristics of *C. latirostris* development. It is worth noticing that, we only analyzed one embryo per day, not being able to contemplate intraspecific differences among embryos of the same stage.

Incubation temperatures under natural conditions vary both within and among nests, and consequently incubation periods are often highly variable (Lang *et al.*, 1989; Piña, 2002). Because reptilian embryonic development is highly dependent of incubation environment (Booth, 2006; Miller *et al.*, 2002), artificial incubation of eggs under constant temperatures minimized such variations. In *C. latirostris*, high temperatures increase development rate, producing shorter incubation time varying from 80.9 ± 3.7 days at 29°C to 69.9 ± 5.1 at 33°C (Piña *et al.*, 2003). In this work, incubation period was shorter than the standard recorded for this species at 31°C (73.4 ± 3.5), but these differences are due to clutch variation (Piña *et al.*, 2003). The development is strongly influenced by temperature, but it can be affected by other variables such as nest humidity (Packard and Packard, 1984), gaseous environment (Warburton *et al.*, 1995), and acid-base balance (Etchberger *et al.*, 1992). The lack of information, as regards such variables and the highly variability of the nesting places in *C. latirostris* (Larriera, 1995), make it difficult to develop accurate models to predict embryos' age in natural nests. Therefore, the value of this study lies on the ability to predict relative age at 31°C or the time that an embryo should be kept at such temperature to reach a specific stage. Although the ability to accurately age embryos from morphologic attributes represents a significant advance not only for embryological studies on *C. latirostris*, but also of any other oviparous reptiles.

METHODS

We artificially incubated one clutch (42 eggs) of *Caiman latirostris*, which was collected from San Cristóbal (Santa Fe province, Argentina). The eggs were removed soon after laying and incubated in constant-temperature incubators (31 ± 0.5)°C, buried in moist vermiculite (four parts water to three parts vermiculite by mass), and covered with hydrated grass. Opaque patch development was a determinant to separate fertile from infertile eggs (Donayo *et al.*, 2002). Temperature was monitored by a HOBO™ Data Logger (Onset Computer Corporation, Pocasset, MA), which was checked every day throughout the incubation period and was located among the eggs. Temperature was selected following the mean temperatures obtained in field nests (Piña, 2002). Nest humidity was not measured, but was assumed to be high (90–100% relative humidity). Eggs were placed in one layer, standing regularly apart to avoid temperature and humidity gradients (Ewert and Nelson, 2003).

Embryos were removed every day for the first 10 days and then every 3 days until hatching. They were fixed in buffered formalin and kept in 70% ethanol. Procedures for obtaining and fixing embryos were derived from Ferguson (1985, 1987). We obtained 30-live embryos, nine hatched, two failed during development, and one died before 1 day of age. The upper two-thirds of the eggshell were removed by cutting the shell with scissors, gently lifting the damaged section, and separating extra-embryonic components adjacent to the margins of the opaque patch. For younger embryos, in which it is difficult to assess heart beat, we assumed they were alive by their translucent and firm appearance after egg removal (dead ones are opaque and flaccid; Webb *et al.*, 1983b).

After embryo dissection from eggs, we proceeded with morphological descriptions and morphometric measures, which varied according to developmental stages. All measurements were collected as straight-line distance, hence curvature of the embryos were not taken into account. These measurements comprised of the following: crown-rump length (CRL); snout-vent length (SVL: only measured on embryos older than 26 days), eye length (EYL: measured between the inner corners of eyelids once they have developed and on embryos older than 17 days), dorsal-cranial length (DCL: measured from the anterior tip of the snout to the median posterior edge of the supraoccipital). On embryos without cranial ossification, the DCL was measured from the anterior tip of the snout to the cranial flexure. The Image Pro-Plus 03.0.1® was used to analyze samples of embryos younger than 27 days, whereas a caliper (precision 0.1 mm) was used for embryos older than 27 days. The CRL, SVL, and DCL were converted into index by dividing these lengths against egg maximum diameter. Embryos were typified according to their external features and an embryological series was established by calibration against Ferguson's (1985, 1987) standard series. Descriptions in bold represent features that were described following other criteria than Ferguson (1985, 1987), but considered important for ageing embryos in *Caiman latirostris*.

Embryos younger than 27 days were dyed with Lugol's solutions to highlight their structures. All descriptions and figures were based on fixed materials; therefore, it was possible that some distortions occurred due to differential dehydration of the tissues. Embryos were examined and classified on the 2nd day of incubation, as the band does not appear before that (Donayo *et al.*, 2002).

Maximum and minimum lengths of both egg and patch were measured. The percentage of the opaque patch coverage was estimated, considering such measurements and both surfaces fit to a rectangular plane. The embryos studied were assigned to a specific embryological stage of Ferguson's standard series.

ACKNOWLEDGMENTS

The authors thank all the crew of Proyecto Yacaré who helped during eggs collection and incubation and J. Gonzalez for drawings. Mark Merchant helped with English revision and comments on the manuscript. This is the contribution # 71 from Proyecto Yacaré.

LITERATURE CITED

Andrews RM. 2004. Patterns of embryonic development. In: Deeming DC, editor. Reptilian incubation: Environment, evolution, and behaviour. Nottingham, UK: Nottingham University Press. pp 75–102.

Andrews RM, Mathies T. 2000. Natural history of Reptilian development: Constraints on the evolution of viviparity. BioScience 50: 227–238.

Beggs K, Young J, Georges A, West P. 2000. Ageing the eggs and embryos of the pig-nosed turtles. Carettochelys insculpta (Chelonia: Carettoclelylidae), from northern Australia. Can J Zool 78: 373–392.

Booth DT. 2006. Influence of incubation temperature on hatchling phenotype in reptiles. Physiol Biochem Zool 79:274–281.

Colbert EH, Mook CC. 1951. The ancestral crocodile *Protosuchus*. Bull Am Mus Nat Hist 97:143–182.

Cretekos CJ, Weatherbee SD, Chen C, Badwaik NK, Niswander L, Behringer RR, Rasweirler JJ. 2005. Embryonic staging system for the short-tailed fruit bat. Carollia perspicillata, a model organism for the mammalian order Chiroptera, based upon timed pregnancies in captive-bred animals. Dev Dyn 233:721–738.

Deeming DC, Ferguson MWJ. 1990. Morphometric analysis of embryonic development in *Alligator mississippiensis*. *Crocodylus johnstoni* and *Crocodylus porosus*. J Zool 221:419–439.

Donayo P, Piña C, Larriera A. 2002. Período de incubación, banda de calcificación, peso de los huevos y desarrollo embrionario de *Caiman latirostris* a tres temperaturas diferentes. In: Larriera A, Verdade LM, editors. La conservación y al manejo de Caimanes y Cocodrilos de América Latina, Vol. 2. Piracicaba, São Paulo, Brazil: C.N. Editora. pp 79–90.

Etchberger CR, Ewert MA, Phillips JB, Nelson CE, Prange HD. 1992. Physiological responses to carbon dioxide in embryonic red-eared slider turtles. Trachemys scripta. J Exp Zoolog 264:1–10.

Ewert M, Nelson C. 2003. Metabolic heating of embryos and sex determination in the American alligator. Alligator mississippiensis. J Therm Biol 28:159–165.

Ferguson MWJ. 1985. Reproductive biology and embryology of the crocodilians. In: Gans C, Billet F, Maderson PFA, editors. Biology of the reptilian, Vol. 14. New York: Wiley. pp 329–491.

Ferguson MWJ. 1987. Post-laying stages of embryonic development in crocodilians. In: Webb GJW, Manolis SC, Whitehead PJ, editors. Wildlife management: Crocodiles and alligators. Chipping Norton, NSW: Surrey Beatty & Sons. pp 427–444.

Hamburger V, Hamilton HL. 1992. A series of normal stages in the development of the chick embryo. Dev Dyn 195:231–272.

Hua TM, Wang CL, Chen BH. 2004. Stages of embryonic development for *Alligator sinensis*. Zool Res 25:263–271.

Joanen T, McNease L. 1991. Incubación de huevos de lagartos. In: King WF, editor. Crianza de Cocodrilos: Información de la Literatura Científica. Gland, Switzerland: Crocodile Specialist Group. IUCN. The World Conservation Union. pp 25–31.

Joanen T, McNease L, Ferguson MWJ. 1987. The effects of egg incubation temperature on post-hatching growth of American Alligators. In: Webb GJW, Manolis SC, Whitehead PJ, editors. Wildlife management of crocodiles and alligators. Chipping Norton, NSW: Surrey Beatty & Sons. pp 533–538.

Lang JW, Andrews HV. 1994. Temperature-dependent sex determination in crocodilians. J Exp Zoolog 270:28–44.

Lang JW, Andrews H, Whitaker R. 1989. Sex determination and sex rations in *Crocodylus palustris*. Am Zool 29:935–952.

Larriera A. 1995. Áreas de nidificación y momento óptimo de cosecha de los huevos de *Caiman latirostris* en Santa Fe, Argentina. In: Larriera A, Verdade LM, editors. La conservación y el manejo de Caimanes y Cocodrilos de América Latina, Vol. 1. Santa Fe, Argentina: Banco Bica. pp 221–232.

Larriera A, Donayo P, Imhof A, Piña C. 1996. Calcification band and embryo development of *Caiman latirostris* eggs incubated at three different temperatures. In: Crocodiles. In: Proceedings of the 13th Working Meeting of the Crocodile Specialist Group. Gland, Switzerland: IUCN-The World Conservation Union. pp 261–268.

Magnusson WE, Taylor J. 1980. A description of developmental stages in Crocodylus porosus for use in ageing eggs in the field. Aust Wildl Res 7:479–485.

Miller SL, Green LR, Peebles DM, Hanson MA, Blanco CA. 2002. Effects of chronic hypoxia and protein malnutrition on growth in the developing chick. Am J Obstet Gynecol 186:261–267.

Packard GC, Packard MJ. 1984. Coupling of physiology of embryonic turtles to the hydric environment. In: Seymour RS, editor. Respiration and metabolism of embryonic vertebrates. Dordrecht, Netherlands: Junk Publishers. pp 99–199.

Piña CI. 2002. Un Estudio del Efecto de la Temperatura de Incubación en la Determinación Sexual y el Primer Año de Crecimiento del Yacaré overo, *Caiman latirostris* (Daudin, 1802). Tesis Doctoral. Facultad de Ciencias Exactas, Físicas y Naturales. U. N. C. Argentina. 76p.

Piña CI, Larriera A, Cabrera MR. 2003. Effect of incubation temperature on incubation period, sex ratio, hatching success, and survivorship in *Caiman latirostris (Crocodylia. Alligatoridae)*. J Herpetol 37:199–202.

Piña CI, Larriera A, Medina M, Webb GJW. 2007. Effects of incubation temperature on the size of *Caiman latirostris (Crocodylia: Alligatoridae)* at hatching and after one year. J Herpetol 41:209–214.

Platt SG, Rainwater TR, McMurry ST. 2003. A simple model for estimating the age of Morelet's crocodile embryos. Herp Rev 34:121–122.

Ramírez-Perilla JA. 2005. Ensayos preliminares de incubación de huevos de *Caiman crocodilus crocodilus* y de oferta tecnológica en condiciones de cosecha en vida silvestre. In: Proceedings de la Reunión Regional de América Latina y el Caribe del Grupo de Especialistas en Cocodrilos (CSG/SSC/IUCN), Santa Fe, Argentina. pp 316–330.

Sierra CL, Rodriguez MA, Ulloa GA, Ruiz-Garranza MP, Galvis G. 1996. Efectos de la temperatura de incubación sobre el crecimiento y desarrollo embrionario de *Caiman crocodilus fuscus*. In: Crocodiles. Proceedings of the 13th Working Meeting of the Crocodile Specialist Group. Gland, Switzerland: IUCN-The World Conservation Union. pp 269–273.

Voeltzkow A. 1899. Beitrage zur Entwicklungsgeschichte der Reptilien. I. Biologie und Entwicklung der ausseren Korperform von *Crocodylus madagascariensis* Grand. Abbandle. Senckenb. Naturf Ges 26:1–150.

Warburton SJ, Hastings D, Wang T. 1995. Responses to chronic hypoxia in embryonic alligators. J Exp Zoolog 273:44–50.

Webb GJW, Beal AM, Manolis SC, Dempsey KE. 1987a. The effects of incubation temperature on sex determination and embryonic developmental rate in *Crocodylus johnstoni* and *C. porosus*. In: Webb GJW, Manolis SC, Whitehead PJ, editors. Wildlife Management: Crocodiles and alligators. Chipping Norton, NSW: Surrey Beatty & Sons. pp 507–531.

Webb GJW, Buckworth R, Manolis SC. 1983b. Crocodylus johnstoni in the Mckinlay River, N.T. VI. Nesting biology. Aust Wildl Res 10: 607–637.

Webb GJW, Buckworth R, Sack GC, Manolis SC. 1983a. An interim method for estimating the age of *Crocodylus porosus* embryos. Aust Wildl Res 10:563–570.

Webb GJW, Choquenot D, Whitehead P. 1986. Nest, eggs and embryonic development of *Carettochelys insculpta* (Chelonia: Carettochelidae) from northern Australia. J Zool 1:512–550.

Webb GJW, Manolis SC, Dempsey KE, Whitehead PJ. 1987b. Crocodilian eggs: A functional overview. In: Webb GJW, Manolis SC, Whitehead PJ, editors. Wildlife Management: Crocodiles and alligators. Chipping Norton, NSW: Surrey Beatty & Sons. pp 417–422.

Whitehead PJ, Webb GJW, Seymour RS. 1990. Effect of incubation temperature on development of *Crocodylus johnstoni* embryos. Physiol Zool 63:949–964.